One-Pot Solvent-Free Synthesis of N,N-Bis(2-Hydroxyethyl) Alkylamide from Triglycerides Using Zinc-Doped Calcium Oxide Nanospheroids as a Heterogeneous Catalyst

Dinesh Kumar [1,*], Chan Hee Park [1,2,*] and Cheol Sang Kim [1,*]

[1]   Department of Bionanosystem Engineering, Chonbuk National University, Jeonju 561756, Korea
[2]   Department of Mechanical Design Engineering, Chonbuk National University, Jeonju 561756, Korea
*   Correspondence: dinesh.tu@gmail.com (D.K.); biochan@jbnu.ac.kr (C.H.P.); chskim@jbnu.ac.kr (C.S.K.);
    Tel.: +82-63-270-4283 (D.K.); +82-63-270-4284 (C.H.P.); +82-63-270-4284 (C.S.K.)

Abstract: *N,N*-Bis(2-hydroxyethyl) alkylamide or fatty acid diethanolamides (FADs) were prepared from a variety of triglycerides using diethanolamine in the presence of different transition metal-doped CaO nanocrystalline heterogeneous catalysts. The Zn-doped Cao nanospheroids were found to be the most efficient heterogeneous catalyst, with complete conversion of natural triglycerides to fatty acid diethanolamide in 30 min at 90 °C. The Zn/CaO nanoparticles were recyclable for up to six reaction cycles and showed complete conversion even at room temperature. The amidation reaction of natural triglycerides was found to follow the pseudo-first-order kinetic model, and the first-order rate constant was calculated as 0.171 min^{-1} for jatropha oil aminolysis. The activation energy (*E*a) and pre-exponential factor (*A*) for the same reaction were found to be 47.8 kJ mol^{-1} and 4.75×10^8 min^{-1}, respectively.

1. Introduction

The rapid depletion of fossil fuel resources and global warming has motivated researchers to expand different technologies that utilize renewable energy sources [1–3]. Natural triglycerides [4,5] and lignocellulosic biomass [6–8] have been converted in various platforms to value-added products. Triglycerides in vegetable oils and animal fats have been used in industries as a feedstock for the preparation of fatty amides, nitriles, amines, and alcohols, which in turn are useful for the preparation of various commodity chemicals such as surfactants and different types of polymers [9].

Fatty acid amides have a wide range of applications, viz. in surfactants, cosmetics, fungicides, lubricants, foam-control agents, water repellents, shampoos, detergents, corrosion inhibitors, and antiblocking agents, in plastics processing technologies [5,10,11]. Fatty acid amides possess better ignition properties than simple esters and hence are more useful in biodiesel development technology [12]. Moreover, fatty acid amide derivatives of natural triglycerides (vegetable oils or animal fats) or fatty acids have been found to be free from sulfur or any other aromatic compounds and thus help to lessen the greenhouse effect, showing an improvement in cetane number and cold flow properties and a beneficial effect on particulate matter emissions [12]. The industrial synthesis of fatty acid amides involves a two-step process: first, the conversion of triglycerides into fatty acid methyl/ethyl esters, followed by a high-temperature treatment to prepare fatty acid amides [5].

Due to their great importance, some methodologies to prepare fatty acid amides from fatty acids or fatty acid alkyl esters or triglycerides through treatments with different amines have been proposed previously [13,14]. At the industrial level, homogeneous catalysts such as sodium ethoxide [15], sodium methoxide [16], and calcium chloride [17] are used for the preparation of fatty acid amides. Enzymes have been frequently reported [18,19] as a heterogeneous catalyst for amidation reactions, though they require a longer reaction duration. In addition, solvent-free conditions [20,21], Sm^{III} complexes [22], Sn^{IV} complexes [23], the Deoxo-Fluor reagent [bis(2-methoxyethyl)amino-sulfur trifluoride] [24], and other chemicals [25] have been utilized to obtain the desired amide. However, a few drawbacks are associated with these methods, viz. low product yields, a longer reaction duration, difficult product separation, a lack of catalyst reusability, a large molar excess of reactants, contamination of the product, and the creation of stoichiometric amounts of undesired products. Therefore, it is necessary to extend new, efficient, environmentally friendly, ecologically correct, and reusable catalytic methods for the amidation of fatty acids and triglycerides [26–28]. In the recent past, heterogeneous catalysts have attracted considerable attention, as they are nonhazardous, have good selectivity and recyclability, and are easy to separate from reaction medium [29–31].

In the present report, zinc-doped CaO, MgO, and ZnO were prepared in nanoparticle form using an incipient-wetness impregnation method and were used as heterogeneous catalysts for solvent-free direct amidation of natural triglycerides. The effect of transition metal ion impregnation on CaO activity and calcination temperature was also studied by preparing a series of catalysts with Fe, Co, Cu, Zn, and Cd doped on CaO.

2. Results and Discussion

2.1. Brunauer–Emmett–Teller (BET) Surface Area and Hammett Indicator Test

The basic strength (pK_{BH+}) and surface area of prepared catalysts were analyzed using the Hammett indicator test and Brunauer–Emmett–Teller (BET) surface area measurement, respectively. The basic strength of CaO was found to be increased from 9.8–10.1 to 11.1–15.0 after 2 wt% doping of Zn, which further increased to a maximum of 18.4 after calcination at 400 °C. However, a further increase in calcination temperature decreased the basic strength. The improvement of the basic strength of CaO after zinc ion doping with an increase in calcination temperature up to 400 °C could have been due to the partial dehydration and strong increase in the surface area [32]. An increase in the Zn ion concentration did not improve the basic strength. However, after Zn doping on MgO and ZnO, the basic strength was increased to the range of 15.0–18.4 (Table 1). The BET surface area was another critical factor that had a direct impact on catalytic efficiency. Bare CaO had a surface area of 3.56 m^2/g, which improved to 16.87 m^2/g after 2 wt% doping of Zn along with calcination at 400 °C. However, calcination at high temperatures, viz. 600 °C and 800 °C, caused a reduction in surface area to 10.12 m^2/g and 5.25 m^2/g, respectively, which could have been due to the sintering of material at high temperatures. The doping of the Zn ion on MgO and ZnO also caused an increase in surface area from 10.4 m^2/g to 14.89 m^2/g and 4.72 m^2/g to 12.13 m^2/g, respectively (Table 1). Hence, the doping of the Zn ion and calcination were critical factors responsible for the increase in basic strength and surface area.

2.2. Structural Analysis of Catalyst

The effect of calcination temperature, Zn ion concentration, and different Zn doping on different metal oxides was studied by powder XRD analysis (Figure 1 and Figure S1 in Supporting Information). The presence of the cubic phase of CaO was confirmed by peaks at 2θ values of 32.27°, 37.47°, 53.89°, and 67.39° (JCPDS (Joint Committee on Powder Diffraction Standards) card no. 821691), as shown in Figure 1a. After zinc doping (2 wt%) and calcination at 200 °C (2-Zn/CaO-200), the cubic phase of CaO was converted into a hexagonal form of $Ca(OH)_2$, as supported by the peaks at 18.05°, 28.6°, 34.17°, 47.17°, 50.78°, and 62.57° (JCPDS 84-1276), as shown in Figure S1a. A further increase in the calcination temperature to 400 °C showed the coexistence of both the cubic and hexagonal phases, which might

have been the reason for the abrupt enhancement in the basic strength of 2-Zn/CaO-400. However, a further increase in calcination temperature to 600 °C showed the presence of only the cubic phase. The increase of the Zn ion concentration had no impact on the structure of Zn/CaO-400 (Figure S1b).

Table 1. Effect of calcination temperature, Zn ion concentration, and different oxides on the basic strength, surface area, and crystallite size. BET: Brunauer–Emmett–Teller.

Catalyst Type	Basic Strength (pK_{BH+})	BET Surface Area (m^2/g)	Average Crystallite Size (nm)*
CaO	$9.8 < pK_{BH+} < 10.1$	3.56	108
2-Zn/CaO-100	$11.1 < pK_{BH+} < 15.0$	4.51	35
2-Zn/CaO-200	$15.0 < pK_{BH+} < 18.4$	6.03	37
2-Zn/CaO-400	$18.4 < pK_{BH+}$	16.87	33
2-Zn/CaO-600	$15.0 < pK_{BH+} < 18.4$	10.12	35
2-Zn/CaO-800	$11.1 < pK_{BH+} < 15.0$	5.25	55
1-Zn/CaO-400	$11.1 < pK_{BH+} < 15.0$	11.72	37
3-Zn/CaO-400	$15.0 < pK_{BH+} < 18.4$	16.24	34
4-Zn/CaO-400	$15.0 < pK_{BH+} < 18.4$	16.54	39
5-Zn/CaO-400	$15.0 < pK_{BH+} < 18.4$	14.36	35
2-Zn/MgO-400	$15.0 < pK_{BH+} < 18.4$	14.89	35
2-Zn/ZnO-400	$15.0 < pK_{BH+} < 18.4$	12.13	38

* on (200) plane by Debye–Scherrer method [33].
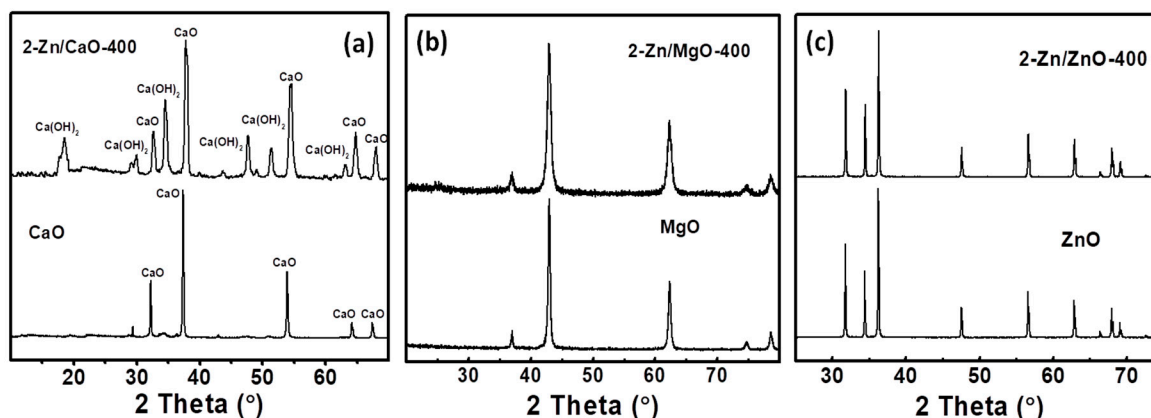
Figure 1. Comparative powder XRD patterns of (**a**) CaO with 2-Zn/CaO-400, (**b**) MgO with 2-Zn/MgO-400, and (**c**) ZnO with 2-Zn/ZnO-400.

XRD patterns for the 2-Zn/MgO-400 catalysts showed sharp diffraction peaks at 2θ = 36.89°, 42.92°, 62.28°, 74.58°, and 78.53°, which were attributed to the crystalline phase of the MgO (JCPDS 4-829) (Figure S1b). The XRD analysis of 2-Zn/ZnO-400 showed the presence of a hexagonal phase of ZnO (JCPDS: 80-0075), as indicated by the peaks at 31.79°, 34.51°, 36.2°, 47.55°, 56.65°, 62.84°, 66.31°, 67.9°, and 69.03° (Figure 1c). The diffraction pattern of Zn was not observed in any XRD spectrum, which might have been due to its high degree of dispersion on CaO/MgO/ZnO or it being below the detection limit of XRD. The particle size of prepared nanoparticles was also calculated from powder XRD analysis data using the Debye–Scherrer method [33]. Bare CaO particles were found to have a 108-nm size, and after Zn doping, it was found to decrease to 33–39 nm in range (Table 1). However, a change in Zn ion concentration and calcination temperature was not found to alter the particle size significantly.

Dynamic light scattering analysis (DLS) was performed for the measurement of the particle size distribution of CaO and 2-Zn/CaO-400 and showed that the average particle size of CaO and 2-Zn/CaO-400 was 115 nm and 35 nm, respectively (Figure 2a,b). The particle size and surface morphology of the prepared catalyst were analyzed through field emission scanning electron microscopy

(FESEM), and the average particle size was observed in the range of 100–200 nm, with irregular surface morphology (Figure 2c). The same particles were analyzed using transmission electron microscopy (TEM) for clear observation of the particle size, and it was found that the 2-Zn/CaO-400 nanoparticles had an average particle size of ~30 nm with an oblate spherical shape (Figure 2d).
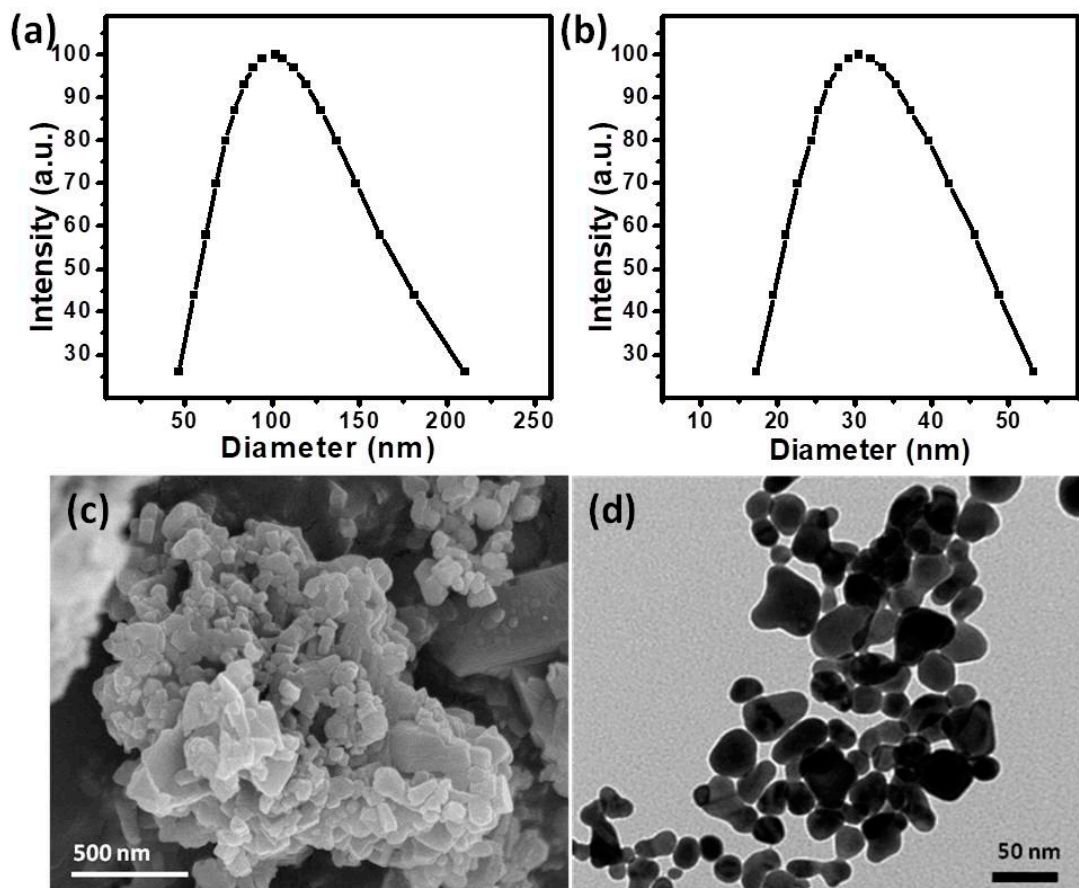
Figure 2. Particle size distributions of (**a**) CaO and (**b**) 2-Zn/CaO-400: (**c**) field emission scanning electron microscopy (FESEM) and (**d**) transmission electron microscopy (TEM) images of 2-Zn/CaO-400.

2.3. Aminolysis Reaction

The amidation of a variety of natural triglycerides, such as virgin soybean oil (VSO), waste soybean oil (WSO), jatropha oil (JO), animal fat (AF), Karanja oil (KO), and fatty acid methyl esters (FAMEs) derived from these oils, as well as methyl laurate (ML) with different molar concentrations of diethanolamine and different catalyst amounts, was performed at 90 °C. All amidation reactions for studying various reaction parameters were carried out with diethanolamine in the presence of 4 wt% of the 2-Zn/CaO-400 catalyst at 90 °C for 0.5 h (Scheme 1). The schematic for the FAMEs derivation from vegetable oils was performed with methanol (9:1 methanol/oil molar ratio) by using 5 wt% of the same catalyst at 65 °C (Scheme S1, Supplementary Materials).

The progress of the amidation reaction was monitored by taking out samples from the reaction mixture and analyzing them with FTIR and ^{1}H-NMR (Nuclear Magnetic Resonance) techniques. The catalyst nanoparticles were removed by simple centrifugation of the final reaction mixture at 7000 rpm, and the organic layer was then washed with distilled water and dried over sodium sulfate. The amide derivatives thus obtained were further analyzed by FTIR (Figure 3A) and ^{1}H-NMR (Figure 1B) analysis techniques. The final reaction product obtained from the methyl laurate amidation reaction was also characterized by mass spectrometry (Figure S4, Supporting Information) along with the ^{1}H-NMR and FTIR studies. A shifting of the ester carbonyl peak to the ester amide peak from 1739 cm^{-1} to

1617 cm^{-1} indicated the formation of fatty acid diethanolamine (FAD) (Figure 3A). The formation of a diethanolamide derivative was also supported by the presence an –OH group peak at 3406 cm^{-1}.
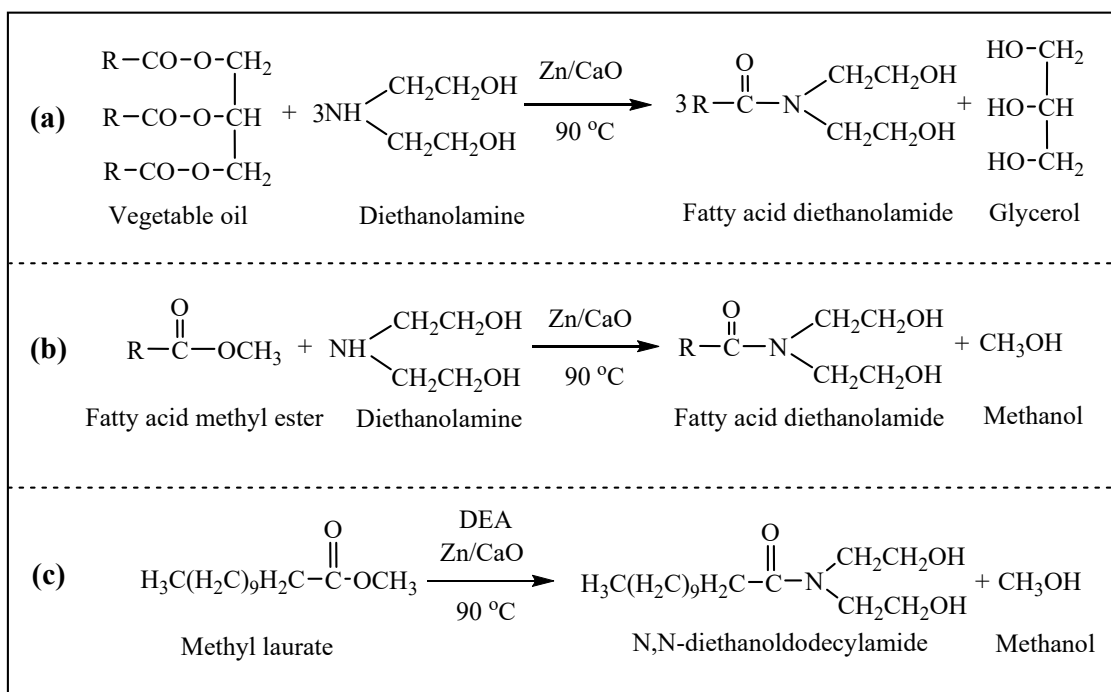

Scheme 1. (**a**) Waste soybean oil or jatropha oil; (**b**) vegetable oil-derived fatty acid methyl esters (FAMEs); and (**c**) methyl laurate-derived fatty acid diethanolamide preparation in the presence of a Zn/CaO solid catalyst.

On the other hand, in the ^{1}H-NMR spectrum, the appearance of a multiplet at 3.48 and 3.78 ppm due to -NCH$_2$- and -CH$_2$OH protons (Figure 3Bb) and the disappearance of characteristic glyceridic proton signals at 4.13 and 4.30 ppm (Figure 3Bi) supported the conversion of triglyceride to corresponding FAD. Furthermore, in the case of a FAD derivative of JO-derived FAMEs and methyl laurate, the disappearance of a methyl ester proton signal at 3.65 ppm (Figure 3Biii,v) and the appearance of amide proton signals at 3.48 and 3.78 ppm (Figure 3Bd,f) (corresponding to -NCH$_2$- and -CH$_2$OH protons) confirmed the formation of respective FAD.

2.3.1. Optimization of Different Parameters

The prepared nanocrystalline catalysts with different transition metals and different metal oxides were utilized for the amidation of natural triglycerides with diethanolamine. However, jatropha oil (JO) was selected for the optimization of parameters, as it has a high level of free fatty acid contents (8.2 wt % free fatty acids).

A series of transition metals was used for the doping in CaO to test their impact on the catalytic activity of CaO for amidation, and it was found that Mn/CaO, Fe/CaO, Co/CaO, Ni/CaO, Cu/CaO, Zn/CaO, and Cd/CaO showed 18%, 24%, 16%, 58%, 15%, 99%, and 25% FADs, which were yielded in 0.5 h at 90 °C. Bare CaO-400 was also tested and was found to have a 10% FAD yield (Figure 4a). Among all the prepared catalysts, Zn/CaO was found to be the most efficient, and it was selected for further optimization studies. Further, for the selection of a metal oxide as a base material, Zn was doped in CaO, MgO, and ZnO, as all of these metal oxides have been extensively reported to be efficient catalysts for different reactions. For the amidation of JO, Zn/CaO was found to be the most effective, with a 99% conversion yield for FADs, whereas Zn/MgO and Zn/ZnO also showed significant conversion rates, with 84% and 76% FAD yields, respectively (Figure 4b). The high surface area was the deciding factor for the catalytic activity.
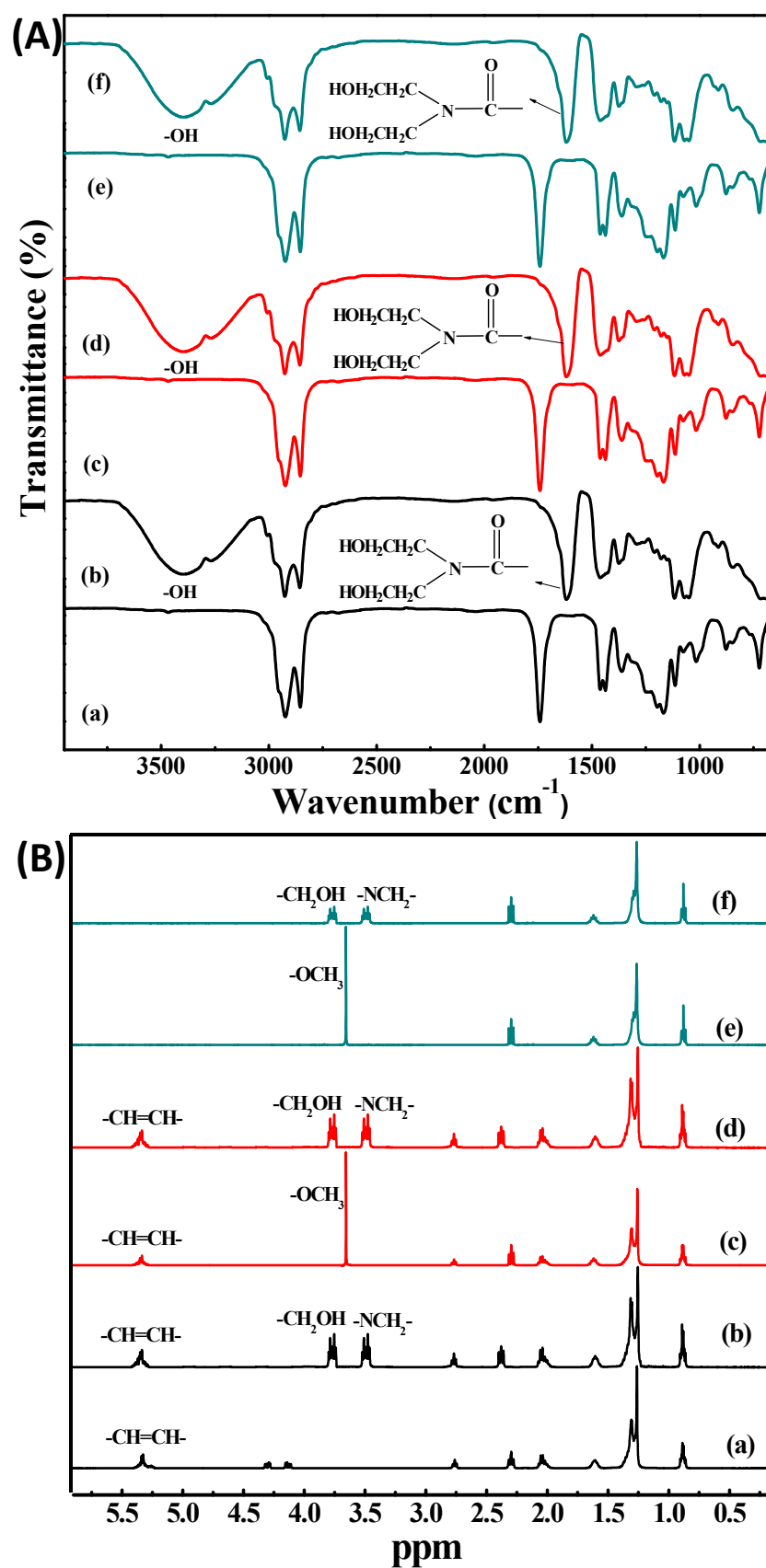
Figure 3. Comparative (**A**) FTIR spectrum and (**B**) ^{1}H-NMR spectrum of (**a**) waste cotton seed oil, (**b**) fatty acid amide of waste cotton seed oil, (**c**) waste soybean oil (WSO)-derived FAMEs, (**d**) a fatty acid amide of WSO-derived FAMEs, (**e**) methyl laurate, and (**f**) an amide derivative of methyl laurate.
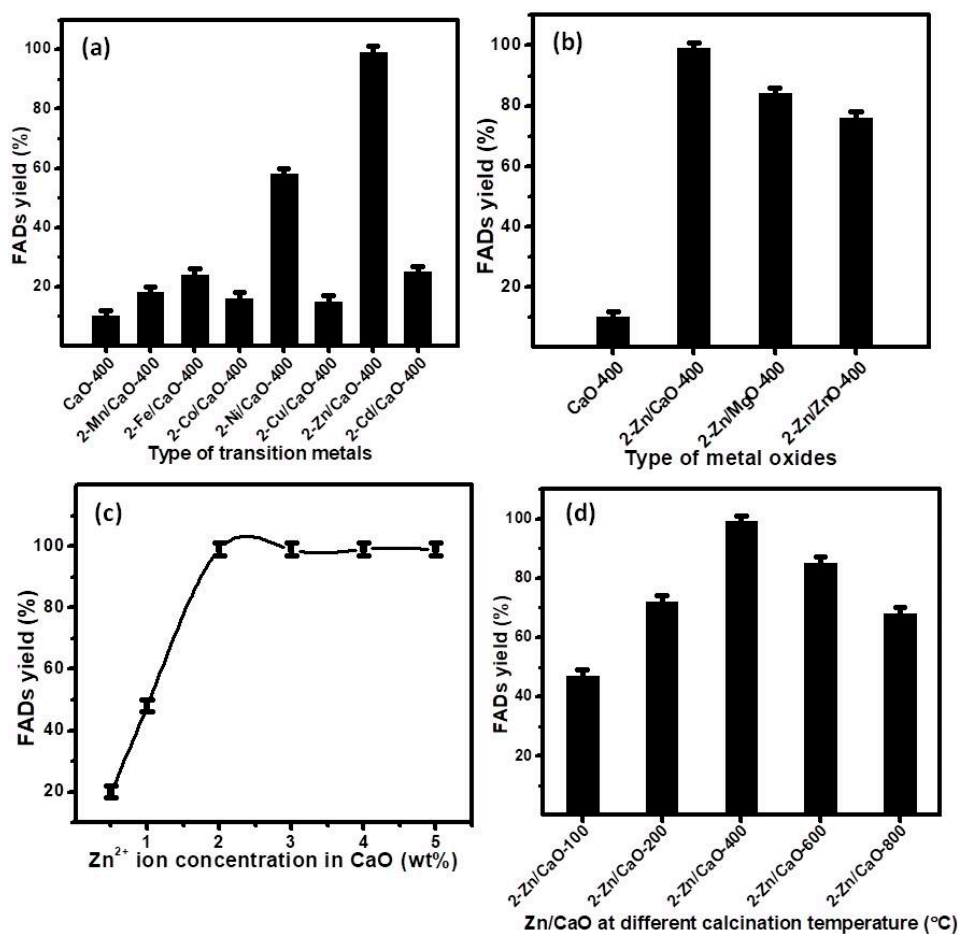
Figure 4. Effect of (**a**) different transition metal doping on CaO, (**b**) Zn ion doping on different metal oxides, (**c**) Zn ion concentration in CaO, and (**d**) calcination temperature in Zn/CaO on the amidation of jatropha oil (JO).

To optimize the concentration of Zn ions for a higher reaction rate, a series of aminolysis reactions was carried out by varying the Zn^{2+} concentration from 0.5 to 5 wt%. There was a significant increase in the FAD yield from 20% to 99%, as the Zn^{2+} concentration increased from 0.5 to 2 wt %, respectively. A further increase in Zn ion concentration had no effect on the reaction rate, and hence 2 wt% was chosen as an optimized amount of Zn for maximum efficiency (Figure 4c). The Zn/CaO nanoparticles prepared at different calcination temperatures were also used for the amidation of JO, and it was observed that the FAD yield was enhanced from 47% to 99% as the calcination temperature increased from 100 to 400 °C, respectively. Interestingly, calcination at a higher temperature such as 600 °C and 800 °C caused a reduction in the reaction rate as the FAD yield lowered to 85% and 68%, respectively. This could have been due to the fact that high temperatures caused the sintering of particles, which in turn decreased the surface area and basic strength (Table 1).

Different catalyst amounts from 1 to 10 wt % and a range of reaction temperatures from 30 to 130 °C were tried to figure out the optimized catalyst amount and reaction temperature. The FAD yield was increased from 25% to 99% when the catalyst amount was enhanced from 1 to 4 wt%. A further increase in the catalyst amount had no impact on the reaction rate (Figure 5a). Similarly, when the reaction temperature was increased from 30 °C to 90 °C, the FAD yield increased significantly from 24% to 99%, respectively. A higher reaction temperature did not show any effect on the reaction rate (Figure 5b). The optimization of the reaction temperature parameter was carried out by taking out samples at 5-, 15-, and 30-min time intervals and analyzing them through FTIR and ^{1}H-NMR analysis.

After 90 °C, there was no change in the reaction rate, and hence 90 °C was used as the optimized reaction temperature.
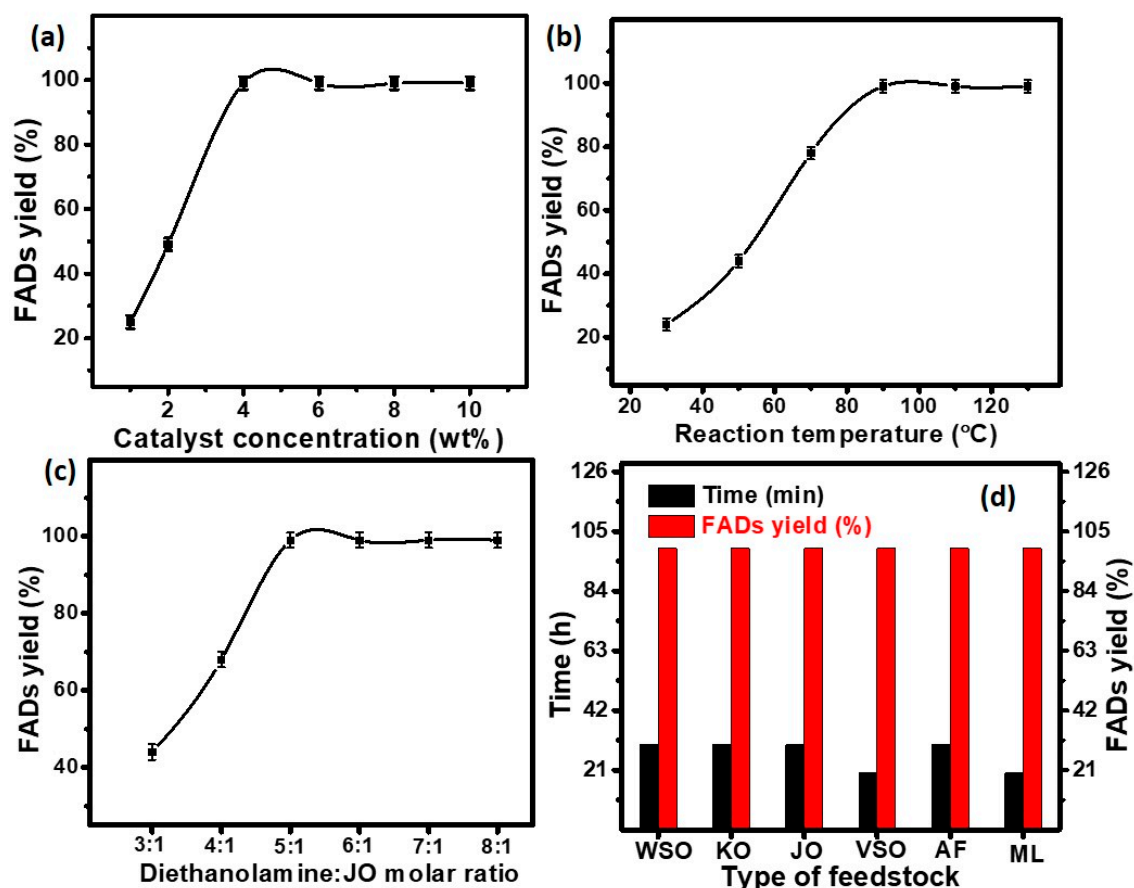
Figure 5. Effect of (**a**) catalyst concentration, (**b**) reaction temperature, and (**c**) the diethanolamine (DEA)/JO molar ratio on the complete aminolysis of used cotton seed oil (reaction time = 0.5 h). (**d**) The effect of different feedstock on the time required and the fatty acid diethanolamine (FAD) yield for the amidation reaction. Reaction conditions: diethanolamine/feedstock = 5:1 (m/m), catalyst amount = 4 wt % of feedstock, temperature = 90 °C.

Six different molar ratios of diethanolamine and JO were used to optimize the diethanolamine (DEA) amount for maximum conversion in the minimum time. As the molar ratio increased from 3:1 to 5:1, the FAD yield also increased from 44% to 99%, respectively, in 0.5 h (Figure 5c). A diethanolamine/JO molar ratio of 5:1, a 4 wt% catalyst amount, and a 90 °C reaction temperature were the final optimum reaction conditions for the complete conversion of JO to fatty acid diethanolamides in the minimum possible time (0.5 h). However, the Zn/CaO nanospheroids were found to convert JO to FADs completely, with a 3:1 diethanolamine/JO molar ratio and a 1 wt% catalyst amount at room temperature (35 °C), but the reaction time increased to 4 h.

A variety of triglycerides, which included natural triglycerides as well as methyl laurate, were tested with an amidation reaction to check the efficiency of the prepared Zn/CaO nanospheroids. Zn/CaO was found to convert all of the triglycerides to FADs, where it took 30 min to complete the reaction in the case of JO, KO, WSO, and AF; and it took only 20 min for VSO and ML. The low free fatty acid (FFA) content was the reason for the lower reaction time for VSO (FFAs = 0.2%) and ML, whereas Zn/CaO was found to be highly efficient for high FFAs containing feedstock, viz. AF (1.4), WSO (2.1), KO (4.4), and JO (8.2). The high FFAs (free fatty acids) caused the partial deactivation of the catalytic sites of Zn/CaO.

To examine the reusability of Zn/CaO nanospheroids, after being recovered from the final reaction mixture through centrifugation, Zn/CaO was washed with hexane and dried at 400 °C. The recovered catalyst was tested for the six catalytic runs under the same reaction conditions and regeneration technique. The recycled and regenerated catalyst was also found to complete (>99 %, m/m) the amidation of JO, though it required 35 min for the second catalytic recycle and 70 min for the sixth catalytic run (Figure S2, Supplementary Materials). The partial loss of catalytic activity could have been due to the loss of Zn/CaO particles during successive centrifugation and the partial leaching of active species.

2.3.2. Kinetic Study

To calculate the reaction rate, the samples from the Zn/CaO-mediated amidation of JO were withdrawn regularly every 10 min and then centrifuged to remove the catalyst; the rotary evaporated was used to remove any remaining amount of diethanolamine; and the samples were finally subjected to FTIR studies to analyze the fatty acid diethanolamide yield. As the reaction progressed, the intensity of the ester carbonyl peak at 1739 cm^{-1} decreased regularly, and the intensity of the fatty acid amide carbonyl band at 1617 cm^{-1} increased due to the conversion of triglyceride to corresponding amide (Figure S3, Supplementary Materials). The amidation of JO in the presence of Zn/CaO was found to follow pseudo-first-order kinetics, and the reaction rate constant (*k*) could be given as

$$k = -\ln\{(1 - X_{FAD})/t\}, \tag{1}$$

where X_{FAD} is the fatty acid diethanolamide yield at time *t*.

The kinetics of the Zn/CaO-catalyzed amidation of JO were studied at a 5:1 diethanolamine/JO molar ratio in the temperature range of 30–90 °C. The linear nature of the $-\ln(1 - X_{FAD})$ versus *t* (time) plots (Figure 6a) supported the idea that the reaction followed pseudo-first-order kinetics. The rate constant values were calculated as 0.171, 0.043, 0.019, and 0.011 min^{-1} at 90, 70, 50, and 30 °C, respectively.
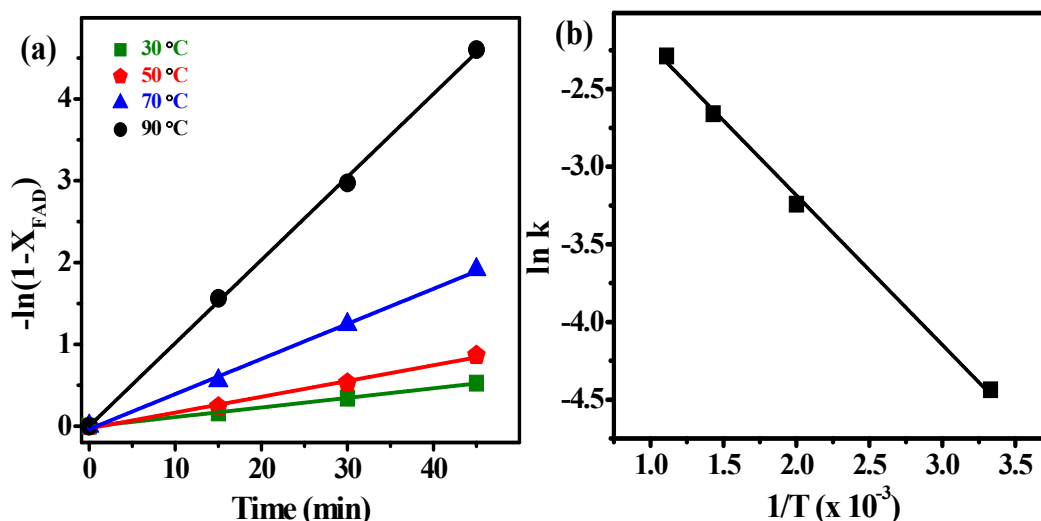
Figure 6. (**a**) Plot of $-\ln(1 - X_{FAD})$ versus *kt* at different reaction temperatures for the 2-Zn/CaO-400-catalyzed aminolysis of JO. (**b**) The Arrhenius equation curve for the aminolysis of JO. Reaction conditions: diethanolamine/JO = 5:1 (m/m), catalyst amount = 4 wt%, temperature = 90 °C.

To calculate the activation energy (E_a) and the pre-exponential factor (*A*) for the amidation reaction, an Arrhenius model was used, as given in Equation (2):

$$\ln k = -E_a/RT + \ln A, \tag{2}$$

where R = the gas constant (8.31 J K^{-1} mol^{-1}), and T is the reaction process temperature in kelvin.

The values of E_a and A calculated from the graph between $1/T$ and ln k were found to be 47.8 kJ mol^{-1} and 4.75×10^8 min^{-1}, respectively (Figure 6b). The resulting activation energy (47.8 kJ mol^{-1}) for the amidation of JO was observed within the range for the heterogeneous catalysis (33–84 kJ mol^{-1}).

3. Materials and Methods

All chemical reagents were purchased from Sigma-Aldrich (St. Louis, MO, USA) and were used without further purification. Transition metal-doped CaO, MgO, and ZnO catalysts were synthesized in nanoparticle form by following a modified incipient-wetness impregnation method.

3.1. General

Nitrates of Mn, Fe, Co, Cu, Ni, Zn, and Cd; zinc acetate; CaO; methanol (99.8%); methyl laurate (99%); and diethanolamine (99%) were purchased from Sigma-Aldrich, USA, and were used as such without further purification. Waste soybean oil was collected from local restaurants located in Jeonju. Scanning electron microscopy (SEM) was performed on a JEOL JSM 6510LV (JEOL Ltd., Akishima, Tokyo, Japan) to collect the SEM images, and transmission electron microscopy (TEM) was performed on a HITACHI 7500 to record TEM images. Scanning microscopy-energy-dispersive X-ray analysis (SEM-EDX) was performed for the qualitative analysis of the catalysts. Fourier-transform–nuclear magnetic resonance (FT–NMR) spectra of vegetable oils, fatty acid methyl esters (FAMEs), and fatty acid amides were recorded on a Bruker Avance-II (400 MHz) spectrophotometer (Bruker Corporation, Billerica, MA, USA). The presence of amide functional groups was supported with the help of FTIR spectra recorded on a Thermo Scientific Nicolet iS10 spectrometer (Thermo Fisher Scientific, Waltham, MA, USA). Mass spectra of methyl laurate and the amide derivative of methyl laurate were recorded on a Waters Micromass Q-ToF Micro mass spectrophotometer (Waters Corporation, Milford, MA, USA) equipped with electrospray ionization (ESI) and atmospheric pressure chemical ionization (APcI) sources with a mass range of 4000 amu in quadruple and 20,000 amu in ToF (Time-Of-Flight). The free fatty acids (FFA), saponification, iodine values, and moisture content of the virgin soybean oil (VSO), animal fat (AF), waste soybean oil (WSO), Karanja oil (KO), and jatropha oil (JO) were determined by following methods reported in the literature [34] (Table S1).

3.2. Experimental Section

3.2.1. Preparation of Catalyst

Transition metal-doped CaO, MgO, and ZnO catalysts were synthesized in nanoparticle form by following a modified incipient-wetness impregnation method [35]. In a typical preparation, metal oxide (CaO or MgO or ZnO) slurry (10 mg/40 mL ethanol) was sonicated for 1 h, and then 10 mL of transition metal (Fe or Co or Cu or Zn or Cd) solution in ethanol of a desired concentration was added dropwise into the metal oxide slurry and stirred moderately for 3 h at 25 °C. The resulting mixture was then dried and calcined at varying temperatures from 100 to 800 °C for 12 h. The solid then obtained was characterized by BET surface area measurement ((ASAP 2010, Micromeritics, USA)), a Hammett indicator test, powder-XRD, DLS (Brookhaven Instruments Corporation, Austin, TX, United States), FESEM, and TEM.

3.2.2. Aminolysis Reaction

Aminolysis reactions of a variety of feedstock (viz. WSO, AF, VSO, KO, and JO), FAMEs derived from them, and methyl laurate (ML) with varying molar concentrations of diethanolamine and catalyst amounts were performed at 90° C. All reactions were carried out until the completion of the reaction by varying one parameter at a time in order to establish the reaction conditions required for complete aminolysis in the minimum possible time. The amide derivative produced during the aminolysis reaction was characterized by FTIR and proton NMR and quantified by FTIR spectroscopy. The amide

derivative of methyl laurate was additionally analyzed using a mass spectroscopic technique. FAMEs prepared through the transesterification of a variety of vegetable oils and mutton fat were characterized and quantified by proton NMR spectroscopy.

Fatty acid amide derivative of WSO: yield > 99%. FTIR (cm^{-1}): 3406 (ν_{OH}), 1617 ($\nu_{C=O}$); ^{1}H-NMR (CDCl$_3$, δ ppm): 5.3 (m, -CH=CH-), 3.77 (m, -CH$_2$OH), 3.46 (m, -NCH$_2$-), 2.7 (m, -CH=CH-CH$_2$-CH=CH-), 2.31 (m, -CH$_2$-CO-), 2.0 (m, -CH$_2$-(CH$_2$)$_n$-CH-), 1.6-1.25 (m, -(CH$_2$)$_n$-), 0.95 (m, -CH=CH-CH$_3$), 0.87 (m, -CH$_2$-CH$_3$).

Fatty acid amide derivative of fatty acid methyl ester of WSO: yield > 99%. FTIR (cm^{-1}): 3406 (ν_{OH}), 1617 ($\nu_{C=O}$); ^{1}H-NMR (CDCl$_3$, δ ppm): 5.3 (m, -CH=CH-), 3.78 (m, -CH$_2$OH), 3.48 (m, -NCH$_2$-), 2.7 (m, -CH=CH-CH$_2$-CH=CH-), 2.3 (m, -CH$_2$-CO-), 2.0 (m, -CH$_2$-(CH$_2$)$_n$-), 1.6-1.25 (m, -(CH$_2$)$_n$-), 0.95 (m, -CH=CH-CH$_3$), 0.87 (m, -CH$_2$-CH$_3$).

Fatty acid amide derivative of animal fat: yield > 99%. FTIR (cm^{-1}): 3406 (ν_{OH}), 1617 ($\nu_{C=O}$); ^{1}H-NMR (CDCl$_3$, δ ppm): 5.34 (m, -CH=CH-), 3.77 (m, -CH$_2$OH), 3.46 (m, -NCH$_2$-), 2.3 (m, -CH$_2$-CO-), 2.0 (m, -CH$_2$-(CH$_2$)$_n$-), 1.6-1.25 (m, -(CH$_2$)$_n$-), 0.87 (m, -CH$_2$-CH$_3$).

Fatty acid amide derivative of fatty acid methyl ester of animal fat: yield > 99%. FTIR (cm^{-1}): 3406 (ν_{OH}), 1617 ($\nu_{C=O}$); ^{1}H-NMR (CDCl$_3$, δ ppm): 5.3 (m, -CH=CH-), 3.75 (m, -CH$_2$OH), 3.47 (m, -NCH$_2$-), 2.3 (m, -CH$_2$-CO-), 2.0 (m, -CH$_2$-(CH$_2$)$_n$-), 1.6-1.25 (m, -(CH$_2$)$_n$-), 0.87 (m, -CH$_2$-CH$_3$).

Fatty acid amide derivative of Karanja oil: yield > 99%. FTIR (cm^{-1}): 3406 (ν_{OH}), 1617 ($\nu_{C=O}$); ^{1}H-NMR (CDCl$_3$, δ ppm): 5.3 (m, -CH=CH-), 3.77 (m, -CH$_2$OH), 3.46 (m, -NCH$_2$-), 2.7 (m, -CH=CH-CH$_2$-CH=CH-), 2.31 (m, -CH$_2$-CO-), 2.0 (m, -CH$_2$-(CH$_2$)$_n$-CH-), 1.6-1.25 (m, -(CH$_2$)$_n$-), 0.95 (m, -CH=CH-CH$_3$)0.87 (m, -CH$_2$-CH$_3$).

Fatty acid amide derivative of fatty acid methyl ester of Karanja oil: yield > 99%. FTIR (cm^{-1}): 3406 (ν_{OH}), 1617 ($\nu_{C=O}$); ^{1}H-NMR (CDCl$_3$, δ ppm): 5.3 (m, -CH=CH-), 3.78 (m, -CH$_2$OH), 3.48 (m, -NCH$_2$-), 2.7 (m, -CH=CH-CH$_2$-CH=CH-), 2.3 (m, -CH$_2$-CO-), 2.0 (m, -CH$_2$-(CH$_2$)$_n$-), 1.6-1.25 (m, -(CH$_2$)$_n$-), 0.95 (m, -CH=CH-CH$_3$), 0.87 (m, -CH$_2$-CH$_3$).

Fatty acid amide derivative of jatropha oil: yield > 99%. FTIR (cm^{-1}): 3406 (ν_{OH}), 1617 ($\nu_{C=O}$); ^{1}H-NMR (CDCl$_3$, δ ppm): 5.3 (m, -CH=CH-), 3.77 (m, -CH$_2$OH), 3.46 (m, -NCH$_2$-), 2.7 (m, -CH=CH-CH$_2$-CH=CH-), 2.31 (m, -CH$_2$-CO-), 2.0 (m, -CH$_2$-(CH$_2$)$_n$-CH-), 1.6-1.25 (m, -(CH$_2$)$_n$-), 0.95 (m, -CH=CH-CH$_3$)0.87 (m, -CH$_2$-CH$_3$).

Fatty acid amide derivative of fatty acid methyl ester of jatropha oil: yield > 99%. FTIR (cm^{-1}): 3406 (ν_{OH}), 1617 ($\nu_{C=O}$); ^{1}H-NMR (CDCl$_3$, δ ppm): 5.3 (m, -CH=CH-), 3.78 (m, -CH$_2$OH), 3.48 (m, -NCH$_2$-), 2.7 (m, -CH=CH-CH$_2$-CH=CH-), 2.3 (m, -CH$_2$-CO-), 2.0 (m, -CH$_2$-(CH$_2$)$_n$-), 1.6-1.25 (m, -(CH$_2$)$_n$-), 0.95 (m, -CH=CH-CH$_3$), 0.87 (m, -CH$_2$-CH$_3$).

Fatty acid amide derivative of methyl laurate: yield > 99%. FTIR (cm^{-1}): 3406 (ν_{OH}), 1617 ($\nu_{amide-C=O}$); ^{1}H-NMR (CDCl$_3$, δ ppm): 3.8 (m, -CH$_2$OH), 3.5 (m, -NCH$_2$-), 2.3 (m, -CH$_2$-CO-), 1.6-1.25 (m, -(CH$_2$)$_n$-), 0.87 (m, -CH$_2$-CH$_3$); EI-MS (electron ionization mass spectrometer) (*m/z*) (intensity (%), fragment): 287.2 (3, M), 270.3 (100, M-H$_2$O), 227.22 (10, M-CH$_3$(CH$_2$)$_3$), 175.2 (10, M-CH$_3$(CH$_2$)$_7$), 132.2 (12, M-CH$_3$(CH$_2$)$_{10}$), 114.2 (5, M-CH$_3$(CH$_2$)$_{10}$OH).

3.2.3. Synthesis of Fatty Acid Methyl Esters

In order to yield FAMEs for aminolysis, the same catalyst was also utilized for the transesterification of a variety of triglycerides (waste cotton seed oil, jatropha oil, and animal fat) with methanol, as shown in Scheme 2. All transesterification reactions were carried out in a refluxing unit consisting of a two-necked round-bottom flask (100 mL) fitted with a water-cooled condenser, an oil bath, and a magnetic stirrer. In a typical transesterification process, vegetable oil or animal fat (triglyceride) was mixed with methanol (in a 9:1 molar ratio with respect to triglyceride) with 5 wt % of Zn/CaO and heated at 65 °C until the completion of the reaction.

The catalyst was removed from the reaction mixture by centrifugation (at 8000 rpm) after the completion of the reaction, the rotary evaporated was used to recover the excess methanol, and then everything was kept in a separate funnel for 12 h to separate the FAMEs from the glycerol. The FAMEs

were thus obtained, further analyzed, and quantified through methods reported in the literature [32] using ^{1}H-NMR data.

The FAMEs were synthesized through the transesterification of a variety of triglycerides with methanol (9:1 methanol/oil molar ratio) by using 5 wt % of the same catalyst at 65 °C (Scheme 2).
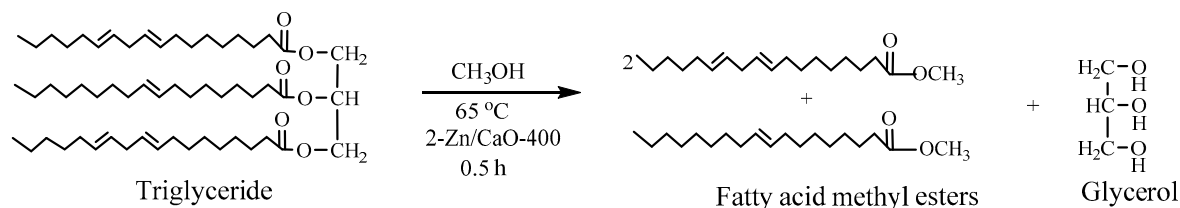
Scheme 2. Transesterification of triglycerides using the 2-Zn/CaO-400 nanocatalyst.

4. Conclusions

Zn-doped CaO nanospheroids were prepared by utilizing a simple method and were used as a heterogeneous catalyst for the amidation of a variety of natural triglycerides. Zn/CaO-400 nanospheroids were found to have a ~30 nm size, more than an 18.4 in basic strength, and 16.87 m^2/g of surface area. All of these factors made it a highly efficient catalyst in amidation, as it took only a 4 wt % catalyst amount for the complete conversion of high FFAs containing JO triglyceride, with a 5:1 molar ratio of DEA/JO at 90 °C. The Zn/CaO nanocatalyst was also found to be efficient at room temperature (35 °C) for amidation reactions of JO. The Zn/CaO-400 nanospheroids were found to be most efficient when compared to other transition metal-doped CaO nanomaterials (Mn, Fe, Co, Ni, Cu, and Cd). In addition, CaO was found to be the most effective support material compared to MgO and ZnO. The presence of both CaO and Ca(OH)$_2$ phases in Zn/CaO-400 made it the most efficient heterogeneous catalyst for the aminolysis of various triglycerides and FAMEs derived from them. Zn/CaO-400 was also found to have excellent recyclability, as it was used for six consecutive reaction cycles without losing much catalytic activity. The high reaction rate of 0.171 min^{-1} with 47.8 kJ mol^{-1} of activation energy and 4.75 X 10^8 pre-exponential factors made it a highly efficient heterogeneous catalyst.

References

1. Kordulis, C.; Bourikas, K.; Gousi, M.; Kordouli, E.; Lycourghiotis, A. Development of nickel based catalysts for the transformation of natural triglycerides and related compounds into green diesel: A critical review. *Appl. Catal. B Environ.* **2016**, *181*, 156–196. [CrossRef]
2. Peng, B.; Yao, Y.; Zhao, C.; Lercher, J.A. Towards quantitative conversion of microalgae oil to diesel-range alkanes with bifunctional catalysts. *Angew. Chem. Int. Ed.* **2012**, *51*, 2072–2075. [CrossRef] [PubMed]
3. Sheldon, R.A. Green chemistry, catalysis and valorization of waste biomass. *J. Mol. Catal. A Chem.* **2016**, *422*, 3–12. [CrossRef]

4.　Besson, M.; Gallezot, P.; Pinel, C. Conversion of biomass into chemicals over metal catalysts. *Chem. Rev.* **2014**, *114*, 1827–1870. [CrossRef] [PubMed]

5.　Pelckmans, M.; Renders, T.; Van de Vyver, S.; Sels, B.F. Bio-based amines through sustainable heterogeneous catalysis. *Green Chem.* **2017**, *19*, 5303–5331. [CrossRef]

6.　Esposito, D.; Antonietti, M. Redefining biorefinery: The search for unconventional building blocks for materials. *Chem. Soc. Rev.* **2015**, *44*, 5821–5835. [CrossRef]

7.　Luterbacher, J.S.; Martin Alonso, D.; Dumesic, J.A. Targeted chemical upgrading of lignocellulosic biomass to platform molecules. *Green Chem.* **2014**, *16*, 4816–4838. [CrossRef]

8.　Tuck, C.O.; Pérez, E.; Horváth, I.T.; Sheldon, R.A.; Poliakoff, M. Valorization of biomass: Deriving more value from waste. *Science* **2012**, *337*, 695–699. [CrossRef]

9.　Foley, P.; Kermanshahi pour, A.; Beach, E.S.; Zimmerman, J.B. Derivation and synthesis of renewable surfactants. *Chem. Soc. Rev.* **2012**, *41*, 1499–1518. [CrossRef]

10.　Biermann, U.; Friedt, W.; Lang, S.; Lühs, W.; Machmüller, G.; Metzger, J.O.; Rüsch gen. Klaas, M.; Schäfer, H.J.; Schneider, M.P. New syntheses with oils and fats as renewable raw materials for the chemical industry. *Angew. Chem. Int. Ed.* **2000**, *39*, 2206–2224. [CrossRef]

11.　Jamil, M.A.R.; Siddiki, S.M.A.H.; Touchy, A.S.; Rashed, M.N.; Poly, S.S.; Jing, Y.; Ting, K.W.; Toyao, T.; Maeno, Z.; Shimizu, K.-i. Selective transformations of triglycerides into fatty amines, amides, and nitriles by using heterogeneous catalysis. *ChemSusChem* **2019**, *12*, 3115–3125. [CrossRef] [PubMed]

12.　Serdari, A.; Lois, E.; Stournas, S. Tertiary fatty amides as diesel fuel substitutes. *Int. J. Energy Res.* **2000**, *24*, 455–466. [CrossRef]

13.　Awasthi, N.P.; Singh, R.P. Microwave-assisted facile and convenient synthesis of fatty acid amide (erucamide): Chemical-catalyzed rapid method. *Eur. J. Lipid Sci. Technol.* **2009**, *111*, 202–206. [CrossRef]

14.　Rawlins, J.; Pramanik, M.; Mendon, S. Synthesis and characterization of soyamide ferulate. *J. Am. Oil Chem. Soc.* **2008**, *85*, 783–789. [CrossRef]

15.　Al-Mulla, E.A.J.; Yunus, W.M.Z.W.; Ibrahim, N.A.B.; Rahman, M.Z.A. Synthesis and characterization of n,n'-carbonyl difatty amides from palm oil. *J. Oleo Sci.* **2009**, *58*, 467–471. [CrossRef] [PubMed]

16.　Yapa Mudiyanselage, A.; Yao, H.; Viamajala, S.; Varanasi, S.; Yamamoto, K. Efficient production of alkanolamides from microalgae. *Ind. Eng. Chem. Res.* **2015**, *54*, 4060–4065. [CrossRef]

17.　Bundesmann, M.W.; Coffey, S.B.; Wright, S.W. Amidation of esters assisted by $Mg(OCH_3)_2$ or $CaCl_2$. *Tetrahedron Lett.* **2010**, *51*, 3879–3882. [CrossRef]

18.　Litjens, M.J.J.; Sha, M.; Straathof, A.J.J.; Jongejan, J.A.; Heijnen, J.J. Competitive lipase-catalyzed ester hydrolysis and ammoniolysis in organic solvents; equilibrium model of a solid–liquid–vapor system. *Biotechnol. Bioeng.* **1999**, *65*, 347–356. [CrossRef]

19.　Wang, X.; Wang, X.; Wang, T. Synthesis of oleoylethanolamide using lipase. *J. Agric. Food Chem.* **2012**, *60*, 451–457. [CrossRef]

20.　Karis, N.D.; Loughlin, W.A.; Jenkins, I.D. A facile and efficient method for the synthesis of novel pyridone analogues by aminolysis of an ester under solvent-free conditions. *Tetrahedron* **2007**, *63*, 12303–12309. [CrossRef]

21.　Sabot, C.; Kumar, K.A.; Meunier, S.; Mioskowski, C. A convenient aminolysis of esters catalyzed by 1,5,7-triazabicyclo[4.4.0]dec-5-ene (tbd) under solvent-free conditions. *Tetrahedron Lett.* **2007**, *48*, 3863–3866. [CrossRef]

22.　Ishii, Y.; Takeno, M.; Kawasaki, Y.; Muromachi, A.; Nishiyama, Y.; Sakaguchi, S. Acylation of alcohols and amines with vinyl acetates catalyzed by cp*2sm(thf)2. *J. Org. Chem.* **1996**, *61*, 3088–3092. [CrossRef] [PubMed]

23.　Chisholm, M.H.; Delbridge, E.E.; Gallucci, J.C. Modeling the catalyst resting state in aryl tin(iv) polymerizations of lactide and estimating the relative rates of transamidation, transesterification and chain transfer. *New J. Chem.* **2004**, *28*, 145–152. [CrossRef]

24.　Kangani, C.O.; Kelley, D.E. One pot direct synthesis of amides or oxazolines from carboxylic acids using deoxo-fluor reagent. *Tetrahedron Lett.* **2005**, *46*, 8917–8920. [CrossRef] [PubMed]

25.　Kumar, K.N.; Sreeramamurthy, K.; Palle, S.; Mukkanti, K.; Das, P. Dithiocarbamate and dbu-promoted amide bond formation under microwave condition. *Tetrahedron Lett.* **2010**, *51*, 899–902. [CrossRef]

26.　Pan, J.; Devarie-Baez, N.O.; Xian, M. Facile amide formation via s-nitrosothioacids. *Org. Lett.* **2011**, *13*, 1092–1094. [CrossRef] [PubMed]

27.   Sasaki, K.; Crich, D. Facile amide bond formation from carboxylic acids and isocyanates. *Org. Lett.* **2011**, *13*, 2256–2259. [CrossRef]

28.   Sathishkumar, M.; Shanmugavelan, P.; Nagarajan, S.; Maheswari, M.; Dinesh, M.; Ponnuswamy, A. Solvent-free protocol for amide bond formation via trapping of nascent phosphazenes with carboxylic acids. *Tetrahedron Lett.* **2011**, *52*, 2830–2833. [CrossRef]

29.   Hayyan, A.; Hashim, M.A.; Hayyan, M. Application of a novel catalyst in the esterification of mixed industrial palm oil for biodiesel production. *BioEnergy Res.* **2014**, *8*, 459–463. [CrossRef]

30.   Kumar, D.; Kim, S.M.; Ali, A. One step synthesis of fatty acid diethanolamides and methyl esters from triglycerides using sodium doped calcium hydroxide as a nanocrystalline heterogeneous catalyst. *New J. Chem.* **2015**, *39*, 7097–7104. [CrossRef]

31.   Lee, A.F.; Bennett, J.A.; Manayil, J.C.; Wilson, K. Heterogeneous catalysis for sustainable biodiesel production via esterification and transesterification. *Chem. Soc. Rev.* **2014**, *43*, 7887–7916. [CrossRef] [PubMed]

32.   Kumar, D.; Ali, A. Transesterification of low-quality triglycerides over a Zn/CaO heterogeneous catalyst: Kinetics and reusability studies. *Energy Fuels* **2013**, *27*, 3758–3768. [CrossRef]

33.   Kumar, D.; Kim, S.M.; Ali, A. Solvent-free one step aminolysis and alcoholysis of low-quality triglycerides using sodium modified cao nanoparticles as a solid catalyst. *RSC Adv.* **2016**, *6*, 55800–55808. [CrossRef]

34.   Kumar, D.; Ali, A. Direct synthesis of fatty acid alkanolamides and fatty acid alkyl esters from high free fatty acid containing triglycerides as lubricity improvers using heterogeneous catalyst. *Fuel* **2015**, *159*, 845–853. [CrossRef]

35.   Degirmenbasi, N.; Boz, N.; Kalyon, D.M. Biofuel production via transesterification using sepiolite-supported alkaline catalysts. *Appl. Catal. B Environ.* **2014**, *150–151*, 147–156. [CrossRef]